A doubly stochastic model for pyroclastic density current hazard assessment: the example of Campi Flegrei caldera

A. Bevilacqua (1,2), A. Neri (1), T. Esposti Ongaro (1), R. Isaia (3),
W. Aspinall (4), P. J. Baxter (5), A. Bertagnini (1), M. Bisson (1), F. Flandoli (6), E. Iannuzzi (3), M. Pistolesi (7), S. Orsucci (1,8), M. Rosi (9), S. Vitale (10)

(1) Istituto Nazionale di Geofisica e Vulcanologia, Sezione di Pisa, Pisa, Italy, (2) Scuola Normale Superiore, Pisa, Italy, (3) Istituto Nazionale di Geofisica e Vulcanologia, Osservatorio Vesuviano, Napoli, Italy, (4) University of Bristol, Bristol and Aspinall and Ass. Trisbury, United Kingdom, (5) University of Cambridge, Institute of Public Health, Cambridge, United Kingdom, (6) Università di Pisa, Dipartimento di Matematica, Pisa, Italy, (7) Università di Firenze, Dipartimento di Scienze della Terra, Firenze, Italy, (8) Università di Pisa, Dipartimento di Fisica, Pisa, Italy, (9) Università di Pisa, Dipartimento di Scienze della Terra, Pisa, Italy, (10) Università di Napoli Federico II, Dipartimento di Scienze della Terra, dell'Ambiente e delle Risorse, Napoli, Italy.

Introduction

Campi Flegrei volcano is assumed as a complex random system that must be assessed with incomplete and uncertain information. In PDC hazard assessment we have to cope with problems affected by a very large uncertainty and for this reason the models constructed are, implicitly, doubly stochastic.

This study includes two main parts, dedicated to different aspects of the volcanic hazard probability assessment at Campi Flegrei caldera, with a particular attention to the uncertainty quantification. The parts correspond to the construction of:

- a map of probability for the location of the next eruptive vent at Campi Flegrei (see also Bevilacqua et al. [2015]);
- a probability distribution for the size of the next PDC, and a map of probability for the PDC invasion hazard at Campi Flegrei (see also Neri et al. [2015]);

The basic idea for a doubly stochastic model is that an observed random variable is modeled in two steps: in one stage, the distribution of the observed outcome is represented using one or more parameters; at a second stage, some of these parameters are treated as being themselves random variables. This raises the definition of a double probability space with two different probability frameworks: one is expected to describe the physical variability of the system (sometimes called aleatoric uncertainty), the other assesses the epistemic uncertainty due to the imperfect knowledge of the system under study.

This distinction is not always easy to do in practice because the two frameworks are correlated and convoluted in producing the available observations, but it is much important because it corresponds to the distinction between an intrinsic randomness of the system and the additional uncertainty that affects its representation, originating from the incomplete information about past behaviour and expressing the degree of belief about alternative assumptions.

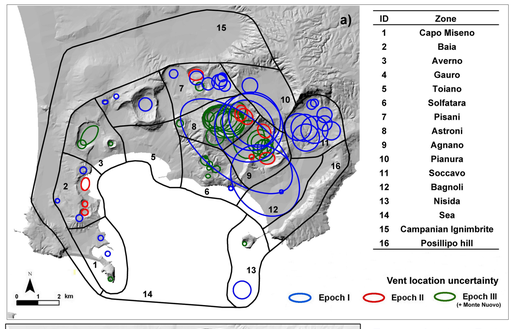

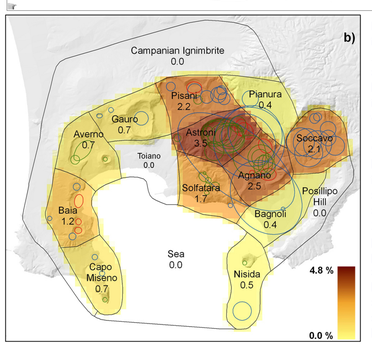

Figure 1. (a) Partitioning of the caldera in 16 zones. The colour of the uncertainty ellipses correspond to the epoch of activity which belong the events. (b) Density distribution of the probability of vent opening from the vent location data distributed homogeneously inside the 16 zones. Values reported indicate the percentage probability of vent opening per km2 (conditional on the occurrence of an eruption). From Bevilacqua et al [2015]

We constructed a background (long-term) spatial map of vent opening probability conditional on the occurrence of an eruption, by incorporating information from some of the most recent studies, specifically focusing on some of the key epistemic uncertainties of the volcanic system. We assumed to express it as a weighted linear combination of the spatial distributions of the relevant variables as the past vent locations during the last 15 ka (reported in Fig. 1), the density of the ground fractures and the density of the faults displacements within the caldera (reported in Fig. 2a and 2b, respectively). With a uniform distribution we also considered the possibility that the probability is correlated with other unknown or neglected variables. The choice of the relative weights and of their uncertainty was based on the expert judgement. In particular it was adopted a simple logic tree (Fig. 3) of questions to whom a group of experts responded; for combining their answers we adopted and compared different performance based elicitation procedures (Cooke [1991]; Flandoli et al. [2010]): also in this case the results were consistent. The probability model that we assumed is doubly stochastic, in the sense that the probability values representing the spatial physical variability affecting the vent opening process are themselves affected by epistemic uncertainty. The sources of epistemic uncertainty considered relate to the uncertain locations of past vents, the incompleteness of the eruptive record, and uncertain weights given to the different volcanic system variables under consideration. Experts judgment outcomes indicate that past vent locations are the most informative factors governing the estimates of the probabilities of vent opening, followed by the locations of faults and fractures (see Tab. 1). Given the approach we have followed, our present results could be modified by eliciting the views of a group of experts composed of those who may hold different views from those who participated in this study, but we would be surprised if their findings diverged greatly from ours when the common basis is the same data, knowledge and process understanding. Our results (Fig. 4) show evidence for a principal high probability region in the central-eastern portion of the caldera characterized by mean probability values of vent opening per km^2 that are about six times greater than the baseline value for the caldera. Significantly lower secondary maxima are found to exist in both the eastern and western parts of the caldera, with probabilities up to about 2-3 times larger than baseline. Nevertheless, the underlying spatial distribution of vent opening position probability is widely dispersed over the whole NYT caldera, including the offshore portion. Most importantly, we accompany our probabilities with quantified epistemic uncertainty estimates which are indicative, typically, of relative spreads ±30% of the local mean value, but with variations between approximately ±10% and ±50%, depending on the location.

The map of vent opening probability

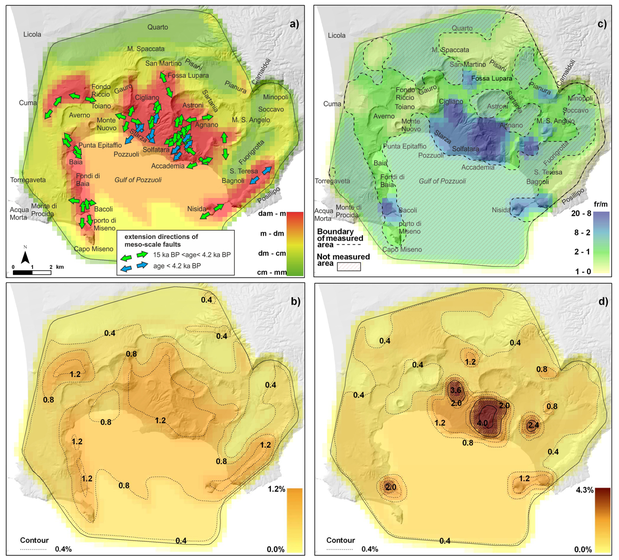

Fig. 2 (a) Distribution of the maximum fault displacement in the caldera. The four colour levels shown correspond to displacements of different orders of magnitude ranging from subcentimetric to metric scales. The figure also shows the extensional directions associated to the main mesoscale faults of the caldera with specific indication of those active in the last 4.2 ka. (b) Density distribution of the probability of vent opening obtained normalizing the values of maximum fault displacement. (c) Distribution of the surface fracture density in the caldera. The four colours correspond to different values of density from about 1 to 20 fractures per meter (fr/m). Wide areas of the inland caldera and the offshore part were not measured (dashed areas). In these areas the average value of the total measured zone was assumed. (d) Density distribution of the probability of vent opening obtained normalizing the values of surface fracture density. From Bevilacqua et al. [2015], derived from the dataset of Vitale and Isaia [2014].

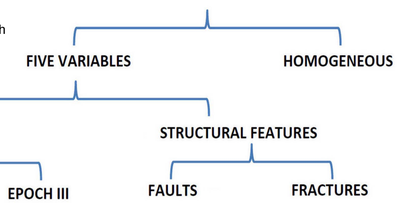

Figure 3. Hierarchical logic tree structure associated to the target questions queried during the elicitation sessions.

Variable/ Statistics	*Vents Epoch I*	*Vents Epoch II*	*Vents Epoch III*	*Lost vents*	*Faults*	*Fractures*	*Homog. map*
5%ile	*6.3*	*1.3*	*10.2*	*3.3*	*8.1*	*5.4*	*6.3*
	9.5	*2.2*	*14.7*	*4.2*	*10.2*	*7*	*8.7*
	6.3	*1.5*	*7.6*	*3.4*	*5.3*	*4.3*	*6.5*
Mean	***16***	***4.5***	***20.4***	***5.9***	***16.4***	***11.9***	***24.9***
	16.4	***4.8***	***22.5***	***6.3***	***16.5***	***12.3***	***21.3***
	17.7	***4.6***	***19.3***	***6.7***	***13.8***	***12***	***25.9***
95%ile	*26.7*	*8.7*	*33.3*	*9*	*26.6*	*20.4*	*42.4*
	24	*7.6*	*31.6*	*8.8*	*23.9*	*18.6*	*31.1*
	30.5	*9.3*	*33.8*	*11*	*24.3*	*22*	*45.4*

Table 1. Probability percentages of the mean and 5th and 95th percentiles of the weight of the five variables considered together with the weights of the lost vents and homogeneous map. The three values reported in each cell refer to, from top to bottom, the CM, ERF and EW models. The median values (i.e. the 50th percentile) are very similar to the mean values, within about 1%.

Figure 4. Probability maps of new vent opening location. Contours and colours indicate the percentage probability of vent opening per km2 conditional on the occurrence of an eruption: (a), (b) and (c) refer to the 5th percentile, mean and 95th percentile values, respectively. Note that for the definition of the PDC invasion maps we do not consider the offshore portion of the caldera as a possible area of vent opening. Modified from Bevilacqua et al. [2015].

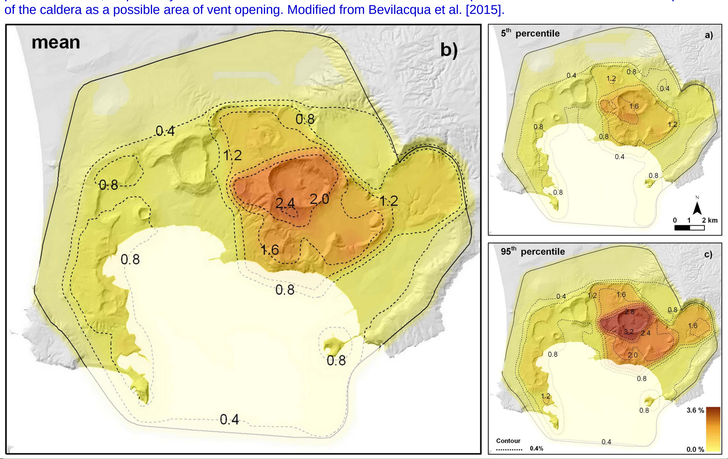

The distribution of PDC invasion areas

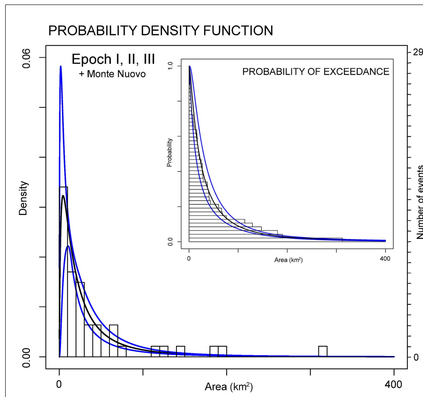

We designated the areas invaded by PDCs as a random variable representative of the aleatoric variability affecting the next eruption event scale. In many cases on-land invasion areas were extended over the sea in order to better represent the total area affected by the flow. The radial underestimation error of deposit boundaries was considered to vary between about 150 and 1,000 m, with a mean value of about 500 m. The recorded inundated areas reported in Tab. 2 were also extended with reasonable estimates for areas of "lost deposits". The spatial extents invaded by these lost PDCs were sampled using a distribution fitted to the available field datasets, truncated with different thresholds. Fig. 5 shows the histograms of PDC invasion areas for the last 15 ka together with the curves of probability density functions derived from them. The class of log-normal distributions appears to be the most appropriate, parameterized by the values of mean and standard deviation: a Monte Carlo simulation implemented calculated the maximum likelihood (ML) parameters for each sample.

Figure 5. Histo-grams of the PDC invasion areas for the last 15 ka. The reported probability density functions include underestimations of PDC run-out and the addition of 'lost deposits'. The box shows the probability exceedance curve (survival function) and its uncertainty range. Modified from Neri et al [2015].

ID	PDC Deposit - Epoch I	Area (km^2)
1	Bellavista Volcano	3.9
2	Mofete Volcano	2.1
3	Gauro Volcano	16.1
4	Santa Teresa Volcano	0.9
5	La Pietra Volcano	2.6
8	Torre Cappella Volcano	1.0
11	Soccavo 1 Tephra	190.5
13	Pomici Principali Tephra	129.2
14	Paleo Pisani 2 Tephra	37.7
16	Soccavo 2 Tephra	75.6
17	Soccavo 3 Tephra	147.5
20	Soccavo 4 Tephra	180.2
21	Paleo San Martino Tephra	37.3
22	Minopoli 2 Tephra	113.6
23	Soccavo 5 Tephra	66.2
25	Pisani 2 Tephra	21.1
28	Montagna Spaccata Tephra	3.0
30	Pisani 3 Tephra	3.0
32	Baccili Volcano	1.1
33	Porto Miseno Volcano	0.7

ID	PDC Deposit - Epoch II	Area (km^2)
2	Fondi di Baia Tephra	15.7
3	Sartania 1 Tephra	40.7
5	Costa San Domenico Tephra	16.9
6	Pigna San Nicola Tephra	8.0
7	Sartania 2 Tephra	27.0
8	San Martino Tephra	19.7

Table 2. Names and invaded area reconstructions for past PDC deposits extended off-shore. From Neri et al. [2015], derived from the dataset of Orsi et al. [2004] with minor modifications .

ID	PDC Deposit - Epoch III	Area (km^2)
2	Agnano 2 Tephra	17.1
3	Averno 1 Tephra	27.0
4	Agnano 3 Tephra	68.0
5	Cigliano Tephra	28.3
7	Capo Miseno Volcano	1.1
8	Monte Sant'Angelo Tephra	43.8
9	Paleoastroni 1 Tephra	18.1
10	Paleoastroni 2 Tephra	5.4
11	Agnano Monte Spina Tephra	312.5
18	Solfatara Tephra	8.7
19	Averno 2 Tephra	24.8
20	Astroni 1 Tephra	39.7
21	Astroni 2 Tephra	19.1
22	Astroni 3 Tephra	41.1
23	Astroni 4 Tephra	60.4
24	Astroni 5 Tephra	29.1
25	Astroni 6 Tephra	26.9
26	Astroni 7 Tephra	10.2
27	Fossa Lupara Tephra	8.9
28	Nisida Tephra	4.7
29	Monte Nuovo Tephra	5.7

The simplified PDC invasion model

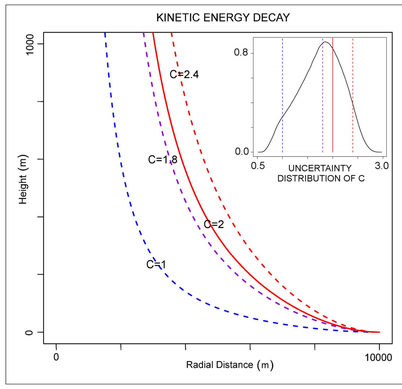

Figure 6. Example of decay of radial flow head kinetic energy expressed in terms of potential height as a function of distance from the source. Curves refer to a flow run-out of 10 km and to values of the C parameter equal to 1.0, 1.8, 2.0, and 2.4 (m$^{2/3}$/s), as re-ported in the labels. In the inset the probability distribu-tion of the C para-meter is shown once a uniform distribution is assumed on the physical variables forming it. From Neri et al . [2015]

A simple integral PDC propagation model is adopted, based on the so called "box model" of Huppert and Simpson [1980]. It allows computation of flow kinematics and of the maximum distance reached over a sub-horizontal surface by a current generated by instantaneous release of a finite volume of gas and particles, at a given concentration. The model has been validated through extensive comparison with 2D numerical simulations produced with the PDAC model (e.g. Neri et al. [2003]). It is applied in an inverse mode, i.e. starting from the invasion areal size and then obtaining the shape of the invaded area, given a specific vent location and surrounding topography. In particular, the flow kinetic energy is compared to the potential energy required to overcome the topographical relief encountered, thus following the same approach of the energy-line model (see Hsu [1975]), but allowing a more realistic description of the propagation of a turbulent flow.

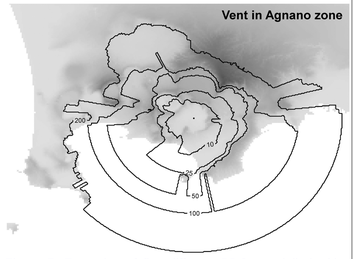

Figure 7. Examples of five different PDCs modelled with the integral emulator from the same vent location, but invading different areal sizes, reported on the contours.

The pyroclastic density current invasion maps

We produced the first quantitative background probabilistic maps of PDC invasion hazard able to incorporate some of the main sources of epistemic uncertainty that influence the models for physical variability (see Fig. 8). In particular, by a Monte Carlo simulation approach we combined the spatial probability distribution of vent opening locations, the inferences about the spatial density distribution of PDC invasion areas informed by reconstruction of deposits from eruptions in the last 15 ka, and the simplified PDC model able to describe the main effect of topography on flow propagation. Our results clearly suggest that the entire caldera has potential to be affected, with a mean probability of flow invasion higher than about 5% and the central-eastern area of the caldera (i.e. Agnano-Astroni-Solfatara) having invasion probabilities above about 30% (with local peaks at or above 50% in Agnano). Significant mean probabilities (up to values of about 10%) are also computed in some areas outside the caldera border (i.e. over Collina di Posillipo and in some neighborhoods of Naples). From our analysis, uncertainty spreads on invasion probabilities inside the caldera typically range between ±15 and ±35% of the local mean value, with an average of about ±25%; wider uncertainties are found outside the caldera, with an average above ±50% and a significantly larger range of variability from place to place. A scientific report about this study have been presented to Dipartimento della Protezione Civile and Commissione Nazionale Grandi Rischi to provide additional information for the definition of the Red Zone at Campi Flegrei.

Figure 8. Example of PDC invasion probability maps computed by assuming the vent opening distribution described in Figure 4 and the density distribution of invasion areas of the last 15 ka, shown in Figure 5. The maps assume that PDCs originate from a single vent per eruption, and that the vent is located in the on-land part of the caldera. Contours and colours indicate the percentage probability of PDC invasion conditional on the occurrence of an explosive eruption. The maps relate to: (b) the mean spatial probability, and to (a) the 5th and (c) 95th percentiles, respectively. Modified from Neri et al. [2015].

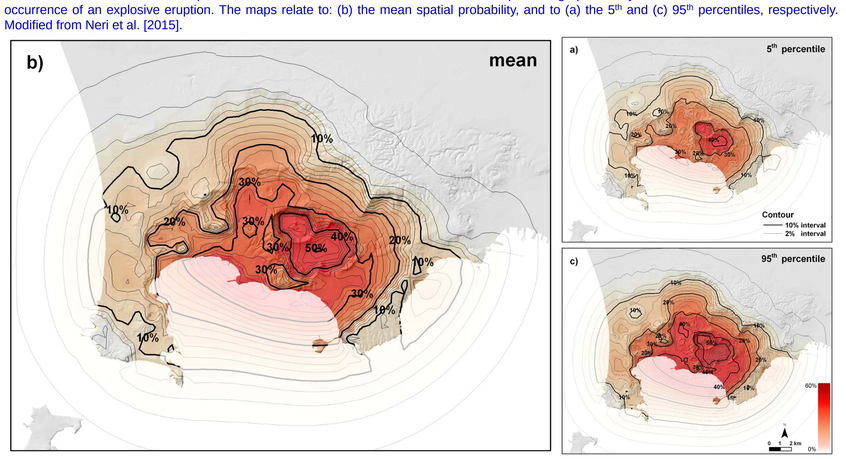

References

Bevilacqua, A., R. Isaia, A. Neri, S. Vitale, W.P. Aspinall, M. Bisson, F. Flandoli, P. J. Baxter, A. Bertagnini, T. Esposti Ongaro, E. Iannuzzi, M. Pistolesi, and M. Rosi (2015), Quantifying volcanic hazard at Campi Flegrei caldera (Italy) with uncertainty assessment: I. Vent opening maps, J. Geophys. Res., doi:10.1002/ 2014JB011775, 120 (4), 2309-2329.

Cooke, R.M. (1991), Experts in Uncertainty: Opinion and Subjective Probability in Science, 336 pp., Oxford Univ. Press, New York.

Flandoli, F., E. Giorgi, W.P. Aspinall and A. Neri (2011), Comparison of a new expert elicitation model with the Classical Model, equal weights and single experts, using a cross-validation technique, Rel. Eng. Syst. Safety, 96, 1292-1311.

Hsu, K.J. (1975), Catastrophic debris streams (sturzstroms) generated by rockfalls, Geological Society of America Bulletin, 86, 129-140.

Huppert, H.E. and J.E. Simpson (1980), The slumping of gravity currents, J. Fluid Mech., 99 (4), 785-799.

Neri, A., T. Esposti Ongaro, G. Macedonio and D. Gidaspow (2003), Multiparticle simulation of collapsing volcanic columns and pyroclastic flows, J. Geophys. Res., 108, 148-227.

Neri, A., A. Bevilacqua, T. Esposti Ongaro, R. Isaia, W.P. Aspinall, M. Bisson, F. Flandoli, P. J. Baxter, A. Bertagnini, E. Iannuzzi, S. Orsucci, M. Pistolesi, M. Rosi, and S. Vitale, (2015), Quantifying volcanic hazard at Campi Flegrei caldera (Italy) with uncertainty assessment: II. Pyroclastic density current invasion maps, J. Geophys. Res., doi:10.1002/2014JB011776, 120 (4), 2330-2349.

Orsi, G., M.A. Di Vito and R. Isaia (2004), Volcanic hazard assessment at the restless Campi Flegrei caldera, Bull. Volcanol., 66, 514-530.

Vitale, S. and R. Isaia (2014), Fractures and faults in volcanic rocks (Campi Flegrei, Southern Italy): insights into volcano-tectonic processes, Int. J. Earth Sci., 103, 801-819, doi:10.1007/s00531-013-0979-0.

Aknowledgements

This work has been partially developed during the projects "V1 - Stima della pericolosità vulcanica in termini probabilistici" and "Speed - Scenari di pericolosità e danno dei vulcani della Campania," funded by Dipartimento della Protezione Civile (DPC) and Regione Campania (Speed). Partial support was also provided by the EU-funded MEDSUV project (grant 308665) and the COST Action Expert Judgment Network (tS1304). The manuscript does not necessarily represent official views and policies of the DPC.